Trap state-assisted electron injection in blue quantum dot light-emitting diode

View Online   Export Citation   CrossMark

Xiangwei Qu,[1,2] Jingrui Ma,[1,2] (ID) Chengwei Shan,[1,2] Pai Liu,[1,2] Aung Ko Ko Kyaw,[1,2] and Xiao Wei Sun[1,2,a] (ID)

AFFILIATIONS

[1]Key Laboratory of Energy Conversion and Storage Technologies (Southern University of Science and Technology),
Ministry of Education, Shenzhen 518055, China

[2]Guangdong University Key Laboratory for Advanced Quantum Dot Displays and Lighting, Guangdong-Hong Kong-Macao Joint
Laboratory for Photonic-Thermal-Electrical Energy Materials and Devices, Shenzhen Key Laboratory for Advanced Quantum Dot
Displays and Lighting, and Department of Electrical and Electronic Engineering, Southern University of Science and Technology,
Shenzhen 518055, China

[a]Author to whom correspondence should be addressed: sunxw@sustech.edu.cn

ABSTRACT

We report trap state-assisted electron injection in a blue quantum dot light-emitting diode (QLED) in this work. By replacing an electron transport layer and a quantum dot emission layer, we identify trap states are indeed on blue quantum dots. We also analyze the equivalent circuit model and the density of trap state distribution by impedance spectroscopy. Furthermore, the trap states induce charge transfer in the blue QLED and lower the device efficiency, suggesting the competition between electron injection and trapping in a working device. Our work shows a distinct electron injection mechanism in blue QLEDs that has not been shown in red and green QLEDs.

Published under an exclusive license by AIP Publishing. https://doi.org/10.1063/5.0104341

Colloidal quantum dot light emitting diodes (QLEDs) have been considered as a strong candidate for next generation flat panel display technology due to their narrow linewidth, high efficiency, and low cost.[1–6] Especially, the color gamut of QLEDs could meet the Rec. 2020 standard. Since its first report, the device efficiency and operation lifetime of the QLED have been improved with extensive efforts.[1–10] For example, the maximum external quantum efficiency of red, green, and blue QLEDs has reached 21.6%, 22.9%, and 20.2%,[3,5] respectively. The operation lifetime T_{95} of red and green QLEDs has reached 7668 and 2500 h,[7,8] respectively, at 1000 cd/m². In particular, the operation lifetime T_{50} of inkjet-printed red and green QLEDs is up to 25 178 and 20 655 h (Ref. 9) at 1000 cd/m², respectively. Despite the fast development of red and green QLEDs, the operational lifetime T_{95} of the blue QLED is only about 100 h (Ref. 10) at 1000 cd/m². Therefore, further improvement in the blue QLED operation lifetime is earnestly needed by the display community.

The QLED usually consists of two electrodes, a hole injection layer, a hole transport layer, a quantum dot (QD) emission layer, and an electron transport layer (ETL). For a working device, electrons and holes are injected from their respective electrode under bias and transport through the charge transport layer, then they are injected into the QD emission layer to form excitons. After exciton recombination

(only the radiative portion), photons would generate and escape from the device.[11] To fabricate a high efficiency device, the charge transport layer should be chosen carefully to match the QD emission layer. For instance, ZnO nanoparticles are commonly employed as an electron transport material in QLEDs, because they have high electron mobility ($\sim 10^{-3}$ cm² v⁻¹ s⁻¹).[12] Moreover, the conduction band maximum (CBM) (~ 4.0 eV) of ZnO nanoparticles is close to that of QDs, which enables efficient electron injection.[12] For hole transport materials, we usually employed TFB or poly[9,9-dioctylfluorene-co-N-[4-(3-methyl-propyl)]-diphenylamine] (TFB) poly(9-vinlycarbazole) (PVK) in QLEDs for their deep highest occupied molecular orbital (HOMO) and matched hole mobility (TFB $\sim 10^{-5}$–10^{-2} cm² v⁻¹ s⁻¹).[12] With the matched charge transport layer, electrons and holes can be injected into the QD layer efficiently and realize charge balance in QLEDs.

Meanwhile, trap states are important in any semiconductor devices, influencing the charge transport and recombination. In fact, there are already a few reports on trap states' influence on charge transport in QLEDs.[13–16] In particular, Wang *et al.* observed that PVK could trap electrons in blue QLEDs, and they inserted a ZnSe-based QD interlayer to suppress the electron leakage path.[13] Chrzanowski *et al.* reported ZnMgO traps mediated hole leakage current in green QLEDs, and they found H_2O could passivate the trap sites and block the hole leakage

path.[14] Kim *et al.* reported that the trap states in ZnO nanoparticles can capture electrons from the electrode and reduce efficient electron transport.[15] In comparison, Lee *et al.* observed sub-bandgap emission in InP QLEDs, which is due to the fact that surface states enhanced hole injection.[16] Meanwhile, there are also reports on trap state assisted non-radiative recombination in QLEDs,[10,13,14,16] where trap states result in exciton quenching and device efficiency reduction.

Unlike red and green QLEDs, electron injection is not sufficient for blue QLEDs, which would degrade the device efficiency and stability.[17] To solve the problem, Zhong *et al.* employed the polyethylenimine (PEI) interlayer to enhance electron injection into the QD emission layer. Correspondingly, the maximum external quantum efficiency (EQE) of blue QLEDs was increased from 2.5% to 5.5%.[18] In our previous work, we inserted an ultra-thin LiF interfacial layer between ZnO nanoparticles and QD layer to facilitate electron tunneling into the QD emission layer.[19] Herein, we report trap state-assisted electron injection in blue QLEDs. In our experiments, trap states can be occupied during a voltage scan. The current density, threshold voltage, and capacitance characteristics of the pristine device suggest clear trap assisted electron injection. We build up equivalent circuit models and analyze the density of trap state distribution of the pristine device by impedance spectroscopy. Our work shows a distinct election injection mechanism in blue QLEDs that has not been shown in red and green QLEDs.

As shown in Fig. 1(a), our blue QLEDs were fabricated with a structure of ITO/PEDOT:PSS/TFB/QD/ZnMgO/Al, where ITO, PEDOT:PSS, TFB, ZnMgO, and Al work as an anode, a hole injection layer, a hole transport layer, an electron transport layer, and a cathode, respectively. The electroluminescence (EL) spectrum of the blue QLED is shown in Fig. 1(b), where we could see a pure blue emission peak at 470 nm with 23 nm linewidth. Figures 1(c) and 1(d) show the current density–voltage (J–V) and luminance–voltage (L–V) characteristics of the pristine blue and electrically aged (EA) devices, respectively. We separate the J–V characteristics of the pristine device into three conduction regions as regions I, II, and III, which represent Ohmic, trap-limited, and space charge limited conduction, respectively.[20] The current density of the pristine device is much larger than that of the EA device in region II. For instance, the current density of the pristine device at 2.3 V is 0.1116 mA/cm^2, which is 13 times higher than that of the EA device (0.0081 mA/cm^2). Moreover, the Ohmic conduction transition voltage V_J of the pristine device (1.8 V) is smaller than that of the EA device (2.3 V), and the current density of the pristine device increases dramatically after V_J with an exponential slope of 2.88, indicating evident trap states involved charge injection.[16,20] In L–V characteristics, the turn on voltage V_T of the pristine device (2.5 V) is smaller than that of the EA device (2.6 V), suggesting that electrons are earlier injected into the CBM of the QD emission layer for the pristine device. Therefore, our results reveal a trap state assisted electron injection mechanism in blue QLEDs.

According to the previous report, non-bonded Zn atoms on the quantum dots surface would leave electron accepting states close to CBM,[16,21,22] which provide a stepwise energy level for electron injection. As illustrated in Fig. 2(a), for the pristine device, electrons can be
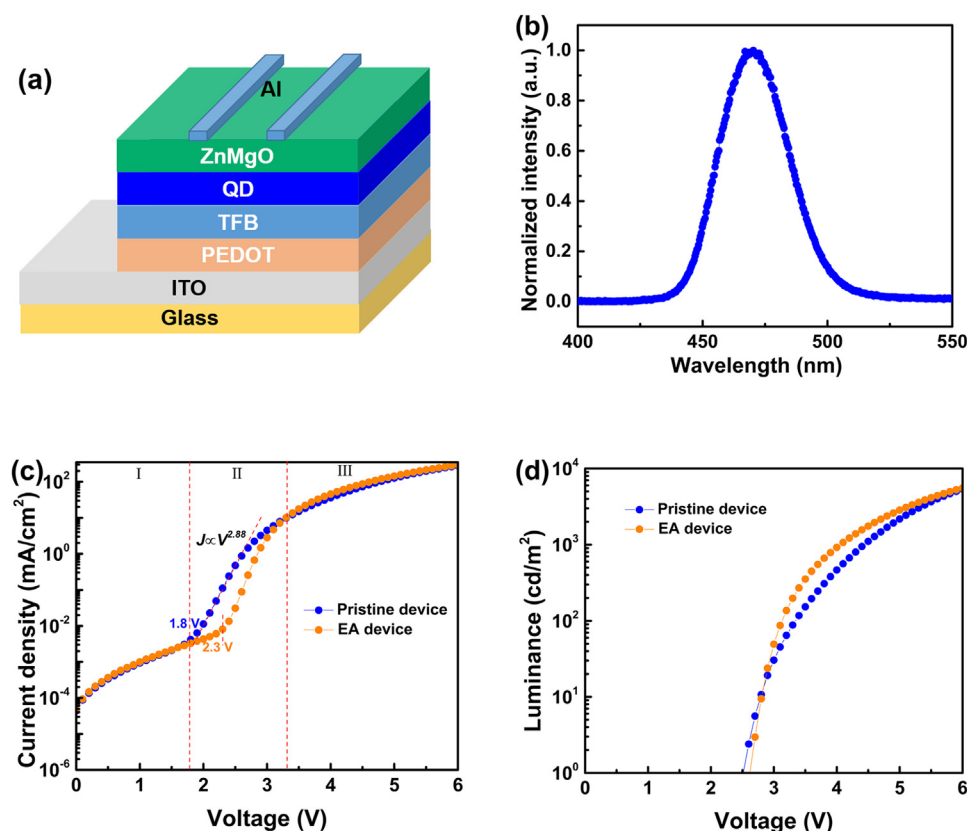
FIG. 1. (a) Device structure and (b) EL spectrum of blue QLEDs; (c) current density–voltage and (d) luminance–voltage characteristics of the pristine device and EA device.
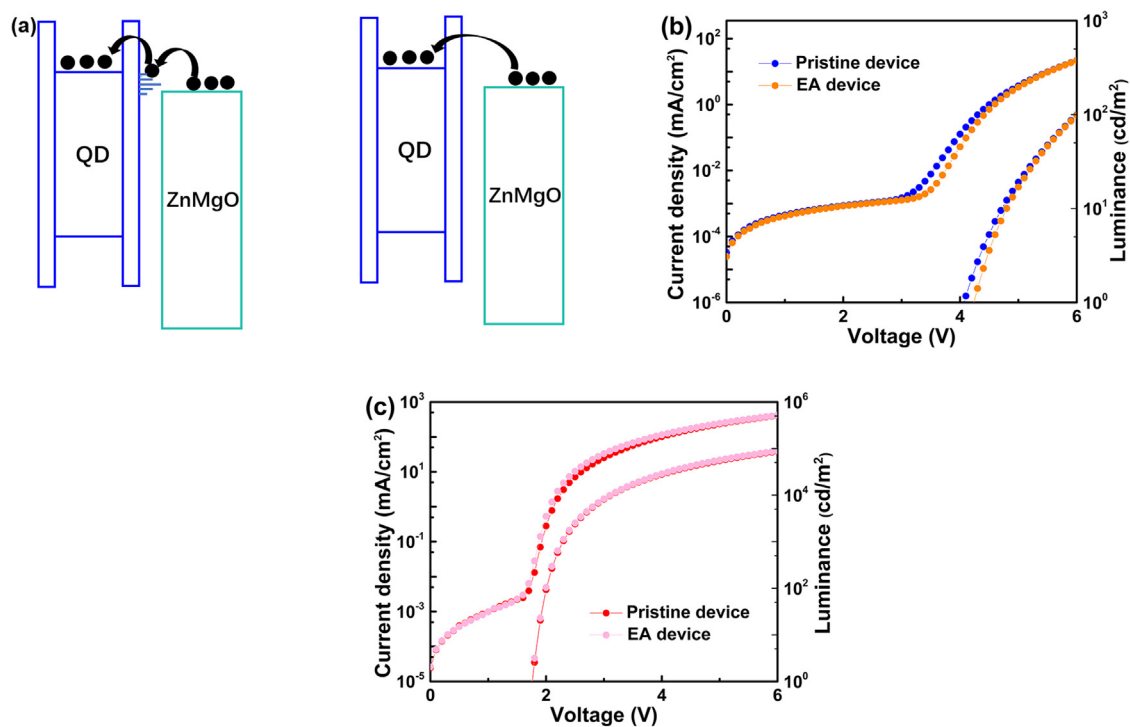
FIG. 2. (a) Diagrams of electron injection in blue QLEDs with or without trap states, (b) J–V and L–V characteristics of (c) blue QLEDs with TPBi ETL, and (d) red QLEDs with ZnMgO ETL.

injected into traps states first, and then further injected into the CBM of QDs with ease. On the other hand, for the EA device, the trap states are occupied during electrical aging, and electrons would be injected into the CBM of QDs directly with a larger injection barrier. Therefore, such a stepwise energy level would facilitate electrons injection into the QD emission layer. To exclude trapping on ZnMgO nanoparticles, we fabricated blue QLEDs employing TPBi as the ETL to replace the ZnMgO nanoparticles. Again, we could still observe the trap state assisted electron injection in the blue QLED with TPBi ETL. As shown in Fig. 2(b), V_J and V_T of the pristine device are smaller than that of the EA device, and the current density of the pristine device is larger than that of the EA device. For comparison purpose, we also fabricated red QLEDs with ZnMgO ETL to check if this trap state assisted electron injection is unique to blue QLEDs. As shown in Fig. 2(c) for the red QLED, the J–V and L–V characteristics of the pristine device are the same as that of the EA device, indicating no/little trap states or their assistance to electron injection is very weak for the red QD case.

Impedance spectroscopy is a useful technique to study charge dynamics in QLEDs.[16,19,23,24] To investigate the trap state assisted electron injection mechanism, the impedance spectroscopy measurement was conducted on blue QLEDs. Figure 3(a) shows the capacitance–voltage (C–V) characteristics of the pristine device and EA device with a frequency of 1 kHz. Under low bias, because little charges are injected into the device, the device capacitance is only contributed by the geometrical capacitance (2.90 nF) and kept unchanged. Then with further increase in bias, owing to electron injection and accumulation

in the device, the capacitance starts to increase.[24] When the device capacitance reaches its peak value, it begins to drop due to electron–hole recombination, which depletes the accumulated carriers. We can see that for the pristine device, the capacitance starts to raise at 1.7 V, which is smaller than that of the EA device (2.4 V), suggesting prior electron injection by trap states. Meanwhile, the voltage for capacitance drop of the pristine device (2.8 V) is also smaller than that of the EA device (2.9 V), indicating earlier electrons injection and exciton recombination of the pristine device. Here, we should notice that the pristine device has not yet emitted any light in the bias range of 1.7–2.4 V. Therefore, electrons are injected into traps states of QDs rather than the CBM of QDs, which causes capacitance increase of the pristine device. We can calculate the amount of electrons captured in trap states through the additional capacitance using the following equation:[25]

$$N_i = \frac{1}{qA} \int_{v_1}^{v_2} [C(v) - C_g] dv, \qquad (1)$$

where N_i is the density of electrons trapped, q is the elementary charge, A is the active area of the device, $C(v)$ is the device capacitance, and C_g is the geometrical capacitance. Here, we take $v_1 = 1.7$ V, $v_2 = 2.4$ V, and the density of accumulated electrons in trap states is calculated to be 8.78×10^{17} cm^{-2}. We can also calculate the amount of accumulated electrons at each bias step by the following equation:[25]

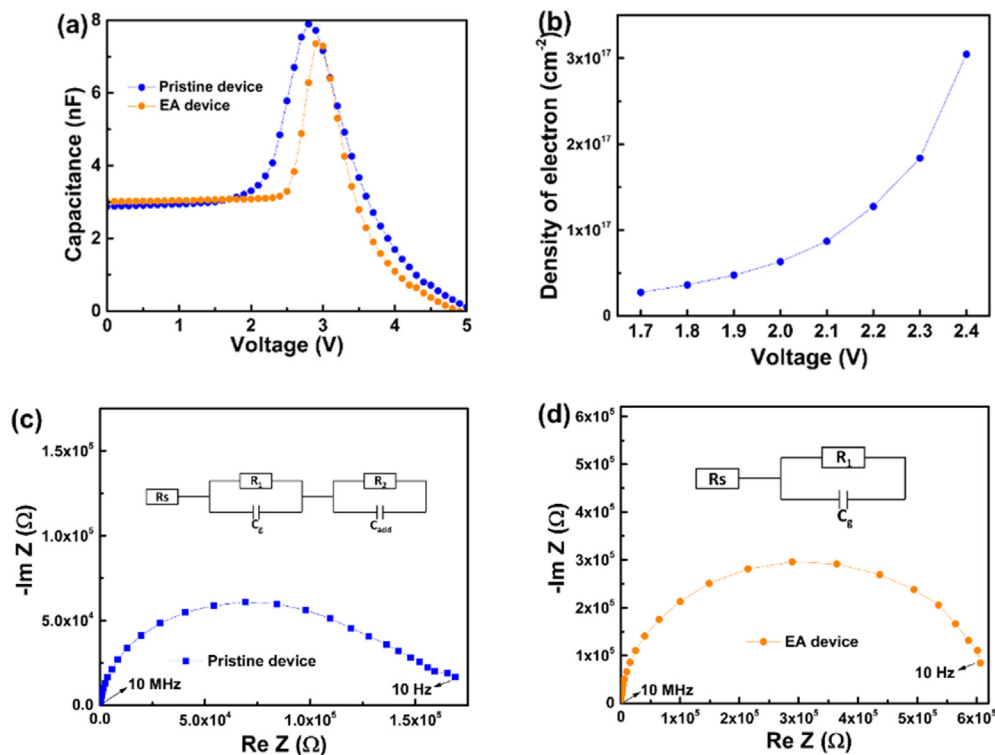$$\Delta N_i = \frac{1}{qA} [C(v) - C_g] \Delta v, \qquad (2)$$

FIG. 3. (a) Capacitance–voltage characteristics of the pristine device and EA device, (b) density of accumulated electrons at the DC voltage, and impedance spectroscopy of the (c) pristine device and (d) EA device at 2.3 V.

where ΔN_i is the density of electrons and $\Delta \nu$ is the bias step. The accumulated electron at each bias is shown in Fig. 3(b), where we can see that more electrons are accumulated in the trap states as the bias increases.

As shown in Fig. 1(c), the current density of the pristine device at 2.3 V is 13 times higher than that of the EA device. To better understand how trap states improve the current density, we build up equivalent circuit models of pristine and EA devices by impedance spectroscopy. Figures 3(c) and 3(d) show the real and imaginary parts of the impedance of the two devices at 2.3 V. The frequency is ranged from 10 Hz to 10 MHz, and the amplitude of the AC signal is 0.1 V. Both devices show semicircle behavior in the Nyquist-plot. As discussed above, the capacitance of the pristine device at 2.3 V consists of geometrical capacitance (C_g) and electron injection induced additional capacitance (C_{add}). Therefore, the semicircle curve of the pristine device is modeled with double RC circuits and a series resistance [Fig. 3(c)]. R_s, R_1, and R_2 are estimated to be 128.2, 1.76×10^5, and 5554 Ω, respectively. C_g and C_{add} are estimated to be 2.98 and 8.47 nF, respectively. For the EA device, the device capacitance is only contributed by C_g, so the semicircle curve of the EA device is modeled with a RC circuit and a series resistance. R_s and R_1 are estimated to be 132.6 and 1.48×10^6 Ω, respectively, and C_g is estimated to be 2.96 nF. According to the fitted data, C_g is close to our experimental data. The total resistance of the pristine device is 1.81×10^5 Ω, which is one order smaller than that of the EA device. Because of this, the electron injection in pristine blue QLEDs is enhanced by the trap states.

Figures 4(a) and 4(b) show the capacitance–frequency characteristics of pristine and EA devices in the frequency range from 10 Hz to 10 MHz. The amplitude of the AC voltage is 0.1 V, and the DC voltage was selected to be 1.7 and 2.3 V. In the high frequency range of 1–10 MHz, the device capacitance is approximately close to 0 F, because the frequency is too high that the charges cannot respond.[23] With the decrease in frequency, the charges can start to follow the AC signal and contribute to the device capacitance. The capacitances of the EA device between 1.7 and 2.3 V are contributed by the geometrical capacitance, indicating little electrons injection into the QD layer (without trap state assistance). The capacitance of the pristine device at 2.3 V increases dramatically as the frequency decreases, suggesting that electrons can follow the AC signal and occupy the trap states that contributes to capacitance raise. In this case, we should notice that, electrons can only follow the AC signal with a frequency of 10 Hz–100 kHz. Therefore, if the angular frequency of the AC signal $\omega \leq \omega_0$ (time constant for charging trap states), electrons can follow the AC signal and occupy the trap states, which would contribute to capacitance raise.[26,27] Thus, time constant for charging the trap states on the QDs is about $\omega_0 = 100$ kHz (Fig. S2). Furthermore, for trap states near the CBM of ZnMgO nanoparticles, electrons can follow the AC signal at relative high frequencies. While for deeper states, a lower frequency is needed to follow the AC signal.[28] Therefore, the capacitance raise of the pristine device is strongly correlated with the density and energy levels
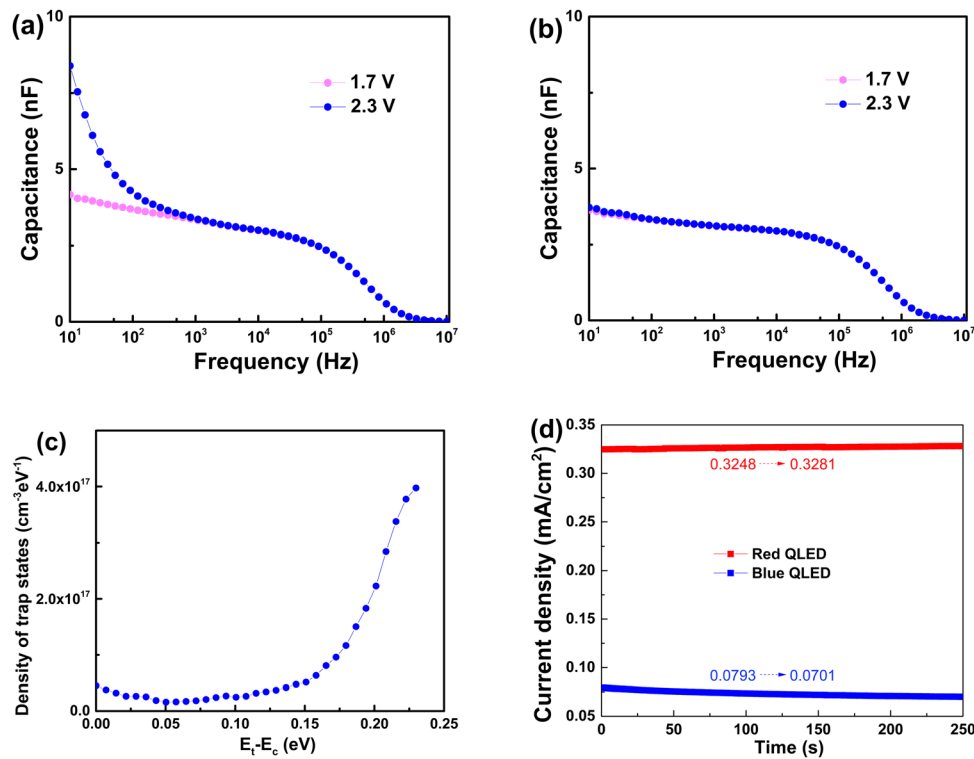
FIG. 4. Capacitance–frequency characteristics of the (a) pristine device and (b) EA device, (c) density of trap states distribution, and (d) electrical aging characteristic of blue (at 2.6 V) and red QLEDs (2 V).

of trap states, which allow us to estimate these parameters using the following equations:[26–28]

$$N_t(\omega) = -\frac{V_{bi}}{qW}\frac{dC}{d\omega}\frac{\omega}{KT}, \qquad (3)$$

$$E(\omega) = KT\ln\frac{\omega_0}{\omega}, \qquad (4)$$

where $N_t(\omega)$ is the density of trap states, V_{bi} is the built-in voltage, q is the elementary charge, W is the depletion width, C is the capacitance, ω is the angular frequency, K is the Boltzmann constant, T is the room temperature, ω_0 is the maximum angular frequency for charging trap states, and $E(\omega)$ is the energy of trap states with respect to the CBM of ZnMgO. Figure 4(c) shows the density of trap state distribution, the energy step used is 0.007 eV, and the density of trap state is around 10^{17} cm^{-3}.

Figure 4(d) compares the electrical aging characteristics of blue and red QLEDs working at a constant bias. The current density of red QLEDs at 2 V increases slightly from 0.3248 to 0.3281 mA/cm^2 due to resistance switching effect of ZnMgO nanoparticles under an electrical field.[29] However, the current density of blue QLEDs at 2.6 V drops continuously from 0.0793 to 0.0701 mA/cm^2. In this case, trap states are gradually occupied under continuous electrical conditioning, and electrons cannot be injected into the QD layer by trap states gradually, causing the drop in the current density. Compared to the resistance switching effect of ZnMgO nanoparticles, the trap states play a dominating role in the charge transport in our experiment here.

On the other hand, the EQE behavior is quite different for the pristine device and EA device. As shown in Fig. 5(a), the EQE of the pristine device increases gradually as the voltage increases. However, for the EA device, it is normal with a small roll-off, which is often observed for red and green QLEDs. At low bias, the EQE of the EA device is much higher than that of the pristine device. For instance, the EQE of the EA device at 3.5 V is 2.42%, which is two times higher than that of the pristine device (1.17%). It is attributed to the electrons transfer by traps in the pristine device. As shown in Fig. 5(b), time resolved photoluminescence (TRPL) is conducted on the pristine device, EA device, and blue QD film. The excitation wavelength of a laser is 405 nm, and the exciton lifetime of the pristine device and EA device is fitted with triple exponential decay, while the exciton lifetime of the blue QD film is fitted with double exponential decay (Table S1). The exciton lifetime of the blue QD film is 3.93 ns; however, it is decreased to 1.99 ns in the pristine device for charge transfer between the QD and charge transfer layer. After electrical aging, the exciton lifetime is recovered to 2.30 ns. For the pristine device, electrons can transfer to the trap states on QDs, which cause exciton quenching. After electrical aging, the trap states are occupied, blocking the electron transfer path, and hence increasing the exciton recombination efficiency, as illustrated in Fig. 5(c). For the EQE characteristics of the pristine device, as the bias increases, the trap states are occupied gradually, which alleviates the exciton quenching, thereby increasing the device efficiency gradually. Finally, the EQE of the pristine device at 6 V is close to that of the EA device. That is to say, trap states act as the electron injection step-stone and electron trapping sites simultaneously in a working device, and there exist competition between electron injection and electron trapping in blue QLEDs.
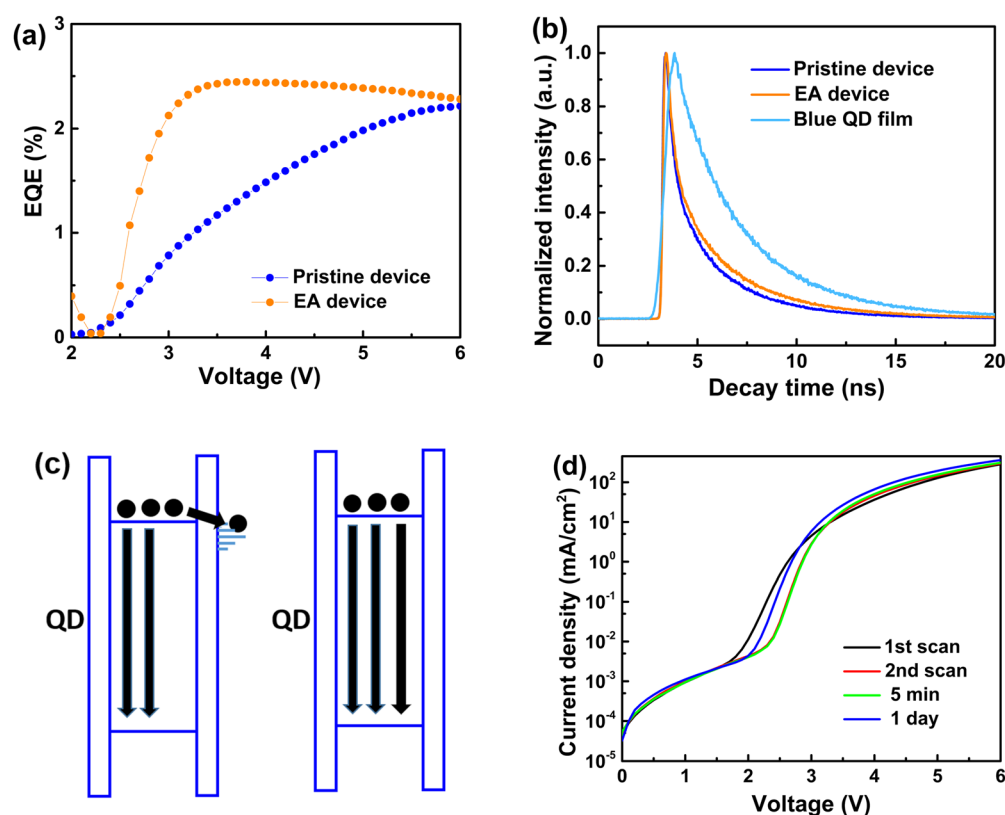
FIG. 5. (a) EQE–voltage characteristics of the pristine device and EA device, (b) TRPL characteristics of the pristine device, EA device, and blue QD film on glass, (c) the electron transfer diagram of blue QDs with or without traps, and (d) current density–voltage characteristics of blue QLEDs at different time.

The trap states on QDs seem to be deep states; as shown in Fig. 5(d), the current density characteristics of the pristine device (first scan) and EA device (second scan) suggest evident trap states assisted electron injection. However, the current density characteristics of blue QLEDs at the voltage scan after 5 min are almost the same with the EA device, i.e., it cannot recover to the current density of the pristine device, indicating a relatively long de-trapping time.[25] Even if we add negative bias on the device, the current density remains unchanged (Fig. S4). The current density is recovered partially, implying electrons located on trap states can be released partially.

In this work, we observed distinct performance of pristine and EA blue QLEDs because of trap assisted electron injection. We employed impedance spectroscopy to analyze the equivalent circuit model and the density of trap state distribution. The trap states also induce charge transfer in a working device and lower the device efficiency, indicating the competition between electron injection and electron trapping in a working device. Our work shows a distinct electron injection mechanism in blue QLEDs related to trap states, which has not been observed in red and green QLEDs. Our work may help us to gradually understand the unusual behavior and much shorter lifetime of blue QLEDs.

See the supplementary material for the experimental section, impedance spectroscopy, capacitance–frequency characteristics, PL spectrum, J–V characteristics of QLEDs, and TRPL fitted data for QLEDs and QD films.

AUTHOR DECLARATIONS
Conflict of Interest

The authors have no conflicts to disclose.

Author Contributions

Xiangwei Qu: Data curation (equal); Investigation (equal); Methodology (equal); Writing – original draft (equal). **Jingrui Ma:** Investigation (equal); Methodology (equal). **Chengwei Shan:** Methodology (equal). **Pai Liu:** Methodology (equal). **Aung Ko Ko Kyaw:** Methodology (equal). **Xiao Wei Sun:** Project administration (equal); Supervision (equal); Writing – review & editing (equal).

DATA AVAILABILITY

The data that support the findings of this study are available from the corresponding author upon reasonable request.

REFERENCES

[1] X. Dai, Z. Zhang, Y. Jin, Y. Niu, H. Cao, X. Liang, L. Chen, J. Wang, and X. Peng, Nature **515**(7525), 96–99 (2014).

[2] W. Cao, C. Xiang, Y. Yang, Q. Chen, L. Chen, X. Yan, and L. Qian, Nat. Commun. **9**(1), 2608 (2018).

[3] H. Shen, Q. Gao, Y. Zhang, Y. Lin, Q. Lin, Z. Li, L. Chen, Z. Zeng, X. Li, Y. Jia, S. Wang, Z. Du, L. S. Li, and Z. Zhang, Nat. Photonics **13**(3), 192–197 (2019).

[4] L. Wang, J. Lin, Y. Hu, X. Guo, Y. Lv, Z. Tang, J. Zhao, Y. Fan, N. Zhang, Y. Wang, and X. Liu, ACS Appl. Mater. Interfaces **9**(44), 38755–38760 (2017).

[5] T. Kim, K. H. Kim, S. Kim, S. M. Choi, H. Jang, H. K. Seo, H. Lee, D. Y. Chung, and E. Jang, Nature **586**(7829), 385–389 (2020).

[6] C. Pu, X. Dai, Y. Shu, M. Zhu, Y. Deng, Y. Jin, and X. Peng, Nat. Commun. **11**(1), 937 (2020).

[7] D. Liu, S. Cao, S. Wang, H. Wang, W. Dai, B. Zou, J. Zhao, and Y. Wang, J. Phys. Chem. Lett. **11**(8), 3111–3115 (2020).

[8] X. Li, Q. Lin, J. Song, H. Shen, H. Zhang, L. S. Li, X. Li, and Z. Du, Adv. Opt. Mater. **8**(2), 1901145 (2020).

[9] S. Jia, H. Tang, J. Ma, S. Ding, X. Qu, B. Xu, Z. Wu, G. Li, P. Liu, K. Wang, and X. W. Sun, Adv. Opt. Mater. **9**(22), 2101069 (2021).

[10] L. Wu, W. Liu, Z. Lu, Y. Yan, J. Zhang, W. Xu, Y. Yang, and X. Yan, SID Symp. Dig. Tech. Pap. **51**(1), 1071–1074 (2020).

[11] Y. Shirasaki, G. J. Supran, M. G. Bawendi, and V. Bulović, Nat. Photonics **7**(1), 13–23 (2013).

[12] H. Shen, Q. Lin, W. Cao, C. Yang, N. T. Shewmon, H. Wang, J. Niu, L. S. Li, and J. Xue, Nanoscale **9**(36), 13583–13591 (2017).

[13] F. Wang, Q. Hua, Q. Lin, F. Zhang, F. Chen, H. Zhang, X. Zhu, X. Xue, X. Xu, H. Shen, H. Zhang, and W. Ji, Adv. Opt. Mater. **10**(13), 2200319 (2022).

[14] M. Chrzanowski, G. Zatryb, P. Sitarek, and A. Podhorodecki, ACS Appl. Mater. Interfaces **13**(17), 20305–20312 (2021).

[15] O.-S. Kim, B.-H. Kang, J.-S. Lee, S.-W. Lee, S.-H. Cha, J.-W. Lee, S.-W. Kim, S.-H. Kim, and S.-W. Kang, IEEE Electron Device Lett. **37**(8), 1022–1024 (2016).

[16] H. Lee, B. G. Jeong, W. K. Bae, D. C. Lee, and J. Lim, Nat. Commun. **12**(1), 5669 (2021).

[17] S. Chen, W. Cao, T. Liu, S. W. Tsang, Y. Yang, X. Yan, and L. Qian, Nat. Commun. **10**(1), 765 (2019).

[18] Z. Zhong, J. Zou, C. Jiang, L. Lan, C. Song, Z. He, L. Mu, L. Wang, J. Wang, J. Peng, and Y. Cao, Org. Electron. **58**, 245–249 (2018).

[19] X. Qu, N. Zhang, R. Cai, B. Kang, S. Chen, B. Xu, K. Wang, and X. W. Sun, Appl. Phys. Lett. **114**(7), 071101 (2019).

[20] B. S. Mashford, M. Stevenson, Z. Popovic, C. Hamilton, Z. Zhou, C. Breen, J. Steckel, V. Bulovic, M. Bawendi, S. Coe-Sullivan, and P. T. Kazlas, Nat. Photonics **7**(5), 407–412 (2013).

[21] S. Biswas, S. Kar, and S. Chaudhuri, J. Phys. Chem. B **109**, 17526–17530 (2005).

[22] X. Wang, J. Shi, Z. Feng, M. Li, and C. Li, Phys. Chem. Chem. Phys. **13**(10), 4715 (2011).

[23] C. Blauth, P. Mulvaney, and T. Hirai, J. Appl. Phys. **125**(19), 195501 (2019).

[24] Z. Wu, P. Liu, X. Qu, J. Ma, W. Liu, B. Xu, K. Wang, and X. W. Sun, Adv. Opt. Mater. **9**(17), 2100389 (2021).

[25] M. Lu, P. d Bruyn, H. T. Nicolai, G.-J. A. H. Wetzelaer, and P. W. M. Blom, Organic Electron. **13**(9), 1693–1699 (2012).

[26] T. Walter, R. Herberholz, C. Müller, and H. W. Schock, J. Appl. Phys. **80**(8), 4411–4420 (1996).

[27] R. Herberholz, M. Igalson, and H. W. Schock, J. Appl. Phys. **83**(1), 318–325 (1998).

[28] C. Xiang, L. Wu, Z. Lu, M. Li, Y. Wen, Y. Yang, W. Liu, T. Zhang, W. Cao, S. W. Tsang, B. Shan, X. Yan, and L. Qian, Nat. Commun. **11**(1), 1646 (2020).

[29] S. Ding, Z. Wu, X. Qu, H. Tang, K. Wang, B. Xu, and X. W. Sun, Appl. Phys. Lett. **117**(9), 093501 (2020).